Optimization of Drone-Based Surface-Wave Seismic Surveys Using a Multiple Traveling Salesman Problem

Hamasato, Yohei
Graduate School of Information Science and Electrical Engineering, Kyushu University

Sakaguchi, Akinori
Research Institute of Advanced Electric Propulsion Aircrafts, Kyushu University : Project Assistant Professor

Tsuji, Takeshi
Department of Systems Innovation, Graduate School of Engineering, The University of Tokyo : Professor

Yamamoto, Kaoru
Faculty of Information Science and Electrical Engineering, Kyushu University : Associate Professor

出版情報：Journal of Robotics and Mechatronics. 35 (2), pp.271-278, 2023-04-20. 富士技術出版株式会社
バージョン：

https://doi.org/10.20965/jrm.2023.p0271

Paper:

Optimization of Drone-Based Surface-Wave Seismic Surveys Using a Multiple Traveling Salesman Problem

Yohei Hamasato*, Akinori Sakaguchi, Takeshi Tsuji***, and Kaoru Yamamoto***

*Graduate School and Faculty of Information Science and Electrical Engineering, Kyushu University
744 Motooka, Nishi-ku, Fukuoka 819-0395, Japan
E-mail: {hamasato.youhei.549@s., yamamoto@ees.}kyushu-u.ac.jp
**Research Institute of Advanced Electric Propulsion Aircrafts, Kyushu University
744 Motooka, Nishi-ku, Fukuoka 819-0395, Japan
E-mail: sakaguchi@ees.kyushu-u.ac.jp
***Department of Systems Innovation, Graduate School of Engineering, The University of Tokyo
7-3-1 Hongo, Bunkyo-ku, Tokyo 113-8656, Japan
E-mail: tsuji@sys.t.u-tokyo.ac.jp
[Received October 30, 2022; accepted December 27, 2022]

In this study, we investigate the problem of finding energy-efficient routes for multiple drones conducting a surface-wave seismic survey. The survey utilizes one seismic source and multiple measurement points spread over a designated area. Each drone carries a seismometer, and is tasked with visiting pre-specified points to take measurements of seismic signals by resting idle on the ground for a set time. Due to this mandatory idling time, their energy consumption is not proportional to the flight distance, nor it is possible to apply standard path minimization algorithms. To address this issue, we establish an energy consumption model for each drone and propose algorithms to optimally allocate points to each drone and generate routes that minimize total energy consumption. The validity of these algorithms is discussed using numerical simulations.

Keywords: multi-drone routing, drone applications in seismic survey, multiple traveling salesman problem, fuzzy *c*-means clustering

1. Introduction

In geological investigations, the S-wave velocity structure is one of the most important measures to understand the terrain properties. A seismic survey is an exploration method for estimating the three-dimensional seismic velocity structure (see **Fig. 1** for the schematic diagrams of a manual and automated surveys). If a surface wave analysis is to be applied, one seismic source system and multiple receivers are deployed, as shown in **Fig. 2**. A large number of seismometers have to be installed over a large area, making conventional manual installation, as shown in **Fig. 1(a)**, a very burdensome operation. Therefore, the use of drone technology to perform this task has been proposed [2], where a single drone carries a seismic source and multiple receivers as shown in **Fig. 3**. However, this is only applicable to small-scale surveys, usually to investigate the geological formations.

In this study, we investigate the feasibility of using multiple drones for large-scale seismic surveys, with approximately 100 measurement points. In our setting, each drone carries one seismometer to multiple pre-specified measurement points, as shown in **Fig. 1(b)**. A seismic source [3] is located at a fixed position and continuously generates controlled oscillations that can be measured by each drone upon landing. The drone must stay at each measurement point for some time in idling mode, i.e., stationary on the ground with the power on, so that the seismometer receives superimposed wave signals to improve the signal-to-noise ratio. This is considered the main challenge of this operation: the required idle time depends on the distance from the seismic source, and can easily exceed 30 minutes when the distance is farther than 500 meters. After each measurement is completed, the drone takes off and moves to the next measurement point. This cycle results in significant power consumption at the expense of the drone's batteries.

Considering these practical constraints in conducting seismic surveys using drones, our aim is to examine the feasibility of a large-scale drone-based seismic survey. For this purpose, we start by formulating the problem based on a multiple traveling salesman problem (mTSP). The TSP aims at finding the shortest possible path for a salesman that visits all the nodes in a graph exactly once and returns to the initial node. It can be applied across many areas in logistics, spanning from the traditional shortest-path formulation [4] to more specific problems such as medical logistics [5] and truck-drone delivery systems [6, 7].

In this study, we develop a tailored algorithm to provide a (sub)optimal path for each drone, focusing on battery consumption. The flight distance, as previously discussed, does not reflect the total energy required to complete a seismic survey cycle owing to the mandatory idling

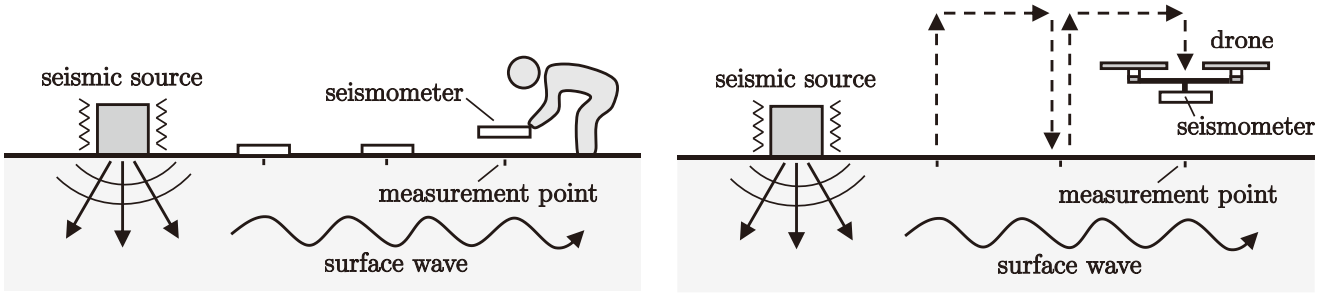

(a) Conventional survey by humans.

(b) Automated survey using a drone with a seismometer.

Fig. 1. Seismic survey types.

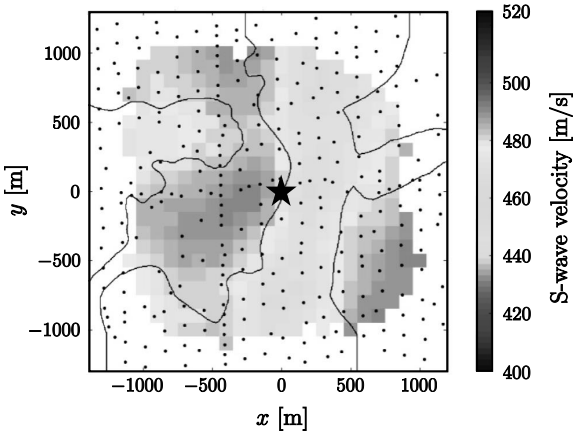

Fig. 2. S-wave velocity structure obtained by a seismic survey. The star and dots show the locations of the seismic source and seismometers, respectively [1].

Fig. 3. Drone with multichannel seismic array [2].

time, in contrast to most TSP-based formulations in logistics that are usually distance-based.

The authors have previously developed two algorithms towards optimizing seismic surveys [8]: while one of them has all drones patrolling without battery recharging, the other considers battery recharging at the starting point. The former method was used to estimate the minimum number of drones required to complete the seismic survey without battery recharging. The latter provides near-optimal routes with recharge planning when the number of drones is limited. In these algorithms, the idling time at each point was set to be the same as the maximum required time in the survey area, regardless of the distance from the seismic source. However, particularly when the survey area is large, the required idling times differ significantly between points closer to and farther away from the source. This study extends the results reported in [8] to accommodate these situations. These algorithms involve solving an mTSP. As in [8], we utilize a heuristic approach based on the method proposed by [9], using the fuzzy c-means clustering [10]. There have been a variety of exact and heuristic solution methods proposed for the mTSP problem, which have been well classified and reviewed in recent extensive surveys, such as [11–13]. Exact methods guarantee the return of an optimal solution with an inevitable curse of dimensionality. Heuristic methods, on the other hand, return a solution within a reasonable time but do not guarantee optimality. By developing an algorithm that is suitable for a particular class of problems, it is possible to obtain a high-quality solution that can be solved in a reasonable computational time. The method reported by [9] returns a solution that equalizes the cost of each salesman. Applying it to the problem addressed by our study, this leads to a shorter survey time and minimized consumed energy, which is beneficial. The developed algorithm is then used for the feasibility study of a drone-based large-scale seismic survey through numerical simulations using the specifications of a commercial drone.

The remainder of this paper is organized as follows. Section 2 defines the problem and energy consumption model for each drone. Based on this model, the proposed algorithms are developed in Section 3 as a three-stage process, with each stage described in a dedicated subsection. Section 4 shows the efficacy of the proposed algorithms using numerical simulations. Section 5 concludes the study.

2. Problem Setting

The problem consists of $n \geq 2$ drones taking off from the same starting point, efficiently visiting $N \gg n$ measurement points, and finally returning to their original point. The starting point is assumed to be a depot with charging facilities, and the seismic source is located there. The index set of drones is denoted as $\mathscr{D} := \{1, \ldots, n\}$ and that of the measurement points as $\mathscr{M} := \{1, \ldots, N\}$. The

preliminary phase of the paths generation plan consists of partitioning the set $\mathscr{M}$ into n mutually disjoint subsets $\mathscr{M}_1, \ldots, \mathscr{M}_n$, each assigned to one drone in such a way that the total energy estimated is minimized. The outcome is used as an educated guess for initialization at a later stage, when energy limitation and battery recharging issues are accounted for.

2.1. Energy Consumption Model

Owing to the mandatory idling step, the energy consumption of each drone is not proportional to their flight distance. To reflect this feature, we consider the following total cost for drone k for moving from measurement points i to j:

$$E_{k,ij} = E_k^{\text{up}} + E_{k,ij}^{\text{fwd}} + E_k^{\text{down}} + E_{k,j}^{\text{idle}}, \quad . \quad . \quad . \quad . \quad . \quad (1)$$

where E_k^{up} and E_k^{down} are the energies consumed by a drone ascending to and descending from a certain position, respectively; $E_{k,ij}^{\text{fwd}}$ is the energy consumed in the forward flight from point i to j; and $E_{k,j}^{\text{idle}}$ is the energy consumed by idling at point j. A suitable height for each drone is assumed to be pre-specified by the user; for example, setting different heights for each drone ensures collision avoidance. We also consider an idling energy $E_{k,j}^{\text{idle}}$ at measurement point j, which is proportional to the distance from the seismic source to point j, taking into account that the surface wave energy is inversely proportional to the distance travelled.

2.2. Energy-Minimizing mTSP Cost Function

The total cost associated with a predefined partition $(\mathscr{M}_1, \ldots, \mathscr{M}_n)$ is given by the sum of all the energy consumed by each drone k when surveying all its assigned measurement points $\mathscr{M}_k$ and flying back to the depot as efficiently as possible. To account for the starting point, an index 0 is assigned to the depot and denote $\overline{\mathscr{M}} := \mathscr{M} \cup \{0\}$ and similarly $\overline{\mathscr{M}}_k := \mathscr{M}_k \cup \{0\}$, $k \in \mathscr{D}$. Additionally, because no idling is necessary at the depot, $E_{k,0}^{\text{idle}} = 0$ is set for all $k \in \mathscr{D}$. Binary variables δ_{ij} are introduced to represent whether a path from point i to j exists ($i, j \in \overline{\mathscr{M}}$); this value is determined as follows:

$$\min_{(\delta_{ij})} \quad E := \sum_{k=1}^{n} \overbrace{\sum_{i,j \in \overline{\mathscr{M}}_k, j \neq i} E_{k,ij}\delta_{ij}}^{:=E_k} \quad . \quad . \quad . \quad . \quad (2a)$$

$$\text{subject to} \quad \sum_{j \in \overline{\mathscr{M}}_k, j \neq i} \delta_{ij} = 1 \quad i \in \overline{\mathscr{M}}_k,\ k \in \mathscr{D} \quad . \quad (2b)$$

$$\sum_{i \in \overline{\mathscr{M}}_k, i \neq j} \delta_{ij} = 1 \quad j \in \overline{\mathscr{M}}_k,\ k \in \mathscr{D} \quad . \quad (2c)$$

$$\delta_{ij} = 0 \quad i \in \mathscr{M}_\ell,\ j \in \mathscr{M}_k,\ \ell \neq k \quad . \quad (2d)$$

$$\delta_{ij} \in \{0,1\} \quad i, j \in \overline{\mathscr{M}}. \quad . \quad . \quad . \quad . \quad (2e)$$

Here, (the optimal value of) E_k is the total energy consumed by drone k starting from the depot, conducting measurements at all its allocated points in $\mathscr{M}_k$, and returning to the depot. Constraint (2c) enforces that each point in $\overline{\mathscr{M}}_k$ is reached exactly once; and Eq. (2b) that one arc leaves from each point exactly once. Together, both constraints ensure that the optimal paths are always closed loops. Constraint (2d) ensures that each drone visits only the points in its assigned cluster, and Eq. (2e) is a binary constraint.

3. Path Generation Algorithms

The paths generation protocol is divided into three stages. The first stage consists of a conventional clustering, which is simply based on the topological distribution of the nodes that have no influence on the energy used. The outcome becomes an educated starting point of a second phase, where each drone is assigned to a cluster in such a way that an evenly distributed total energy consumption across the entire drone fleet is achieved, based on model (2). After the cluster optimization in this second stage, the clusters are no longer modified. The algorithm then generates the optimal trajectories for each drone, by considering their battery capacity, in the third and final stages, generating multiple loops through the depot for recharging as needed. Each of these stages is discussed in separate subsections. The general framework is similar to that proposed in [8]. To better accommodate the distance-based idling time, this study further introduces a suitable weighting and area geometry coefficient for initial area clustering, which is elaborated in the next section.

3.1. Initial Area Clustering

We start by dividing the N measurement points into n areas using the fuzzy c-means clustering method. Unlike hard-clustering methods, which assign each data point to only one cluster, this method allows each data point to belong to multiple clusters with different degrees of membership. For example, a data point that lies close to the centroid of a cluster has a high degree of membership, but possibly it also belongs to other clusters with lower degrees of membership. Departing from the original method [10] and our previous method [8], herein we introduce weights w_i, as in Eq. (3), to prioritize corner areas. The choice of the weights is based on the seismic source (and starting point) being located around the centroid of all measurement points. To cover more remote corners, the coefficient $\gamma \geq 1$ is also a novelty introduced in this model, which is used to control how the position of the centroids spreads farther from each other and from the centroid of the entire area. As a successful heuristic in our experiments, $\gamma = 1.4$.

This flexibility is exploited in the second stage, which is discussed in the next subsection, and aims at equalizing the energy consumption across each drone as much as possible towards reducing the total survey time. For this reason, it is advantageous not to strictly assign each point to a single area during the initial clustering phase because there is room to further optimize the energy consumption of each drone during the path generation phase. This point is further clarified below.

The fuzzy c-means clustering method is formulated according to the following minimization problem:

$$\text{minimize} \;\; J_\alpha(\boldsymbol{U}, \boldsymbol{p}_\mathrm{a}) \coloneqq \sum_{k=1}^{n}\sum_{i=1}^{N}(u_{ki})^\alpha \|\boldsymbol{p}_{\mathrm{m},i} - \boldsymbol{p}_{\mathrm{a},k}\|^2$$

$$\text{subject to} \;\; \sum_{k=1}^{n} u_{ki} = 1, \; i = 1, \ldots, N,$$

where $\boldsymbol{p}_{\mathrm{a},k} \in \mathbb{R}^2$ is the centroid of area k in the coordinate system $\mathscr{F} = (\boldsymbol{e}_x, \boldsymbol{e}_y)$, $\boldsymbol{p}_\mathrm{a} = [\boldsymbol{p}_{\mathrm{a},1}^\top \cdots \; \boldsymbol{p}_{\mathrm{a},n}^\top]^\top \in \mathbb{R}^{2n}$, and $\boldsymbol{p}_{\mathrm{m},i} \in \mathbb{R}^2$ denotes the position of point i. $u_{ki} \in \mathbb{R}$ defines the membership degree of point i to area k and $\boldsymbol{U} \coloneqq [u_{ki}] \in \mathbb{R}^{n\times N}$. The membership degree u_{ki} lies in the interval $[0,1]$. The closer the membership degree is to 1, the stronger the point belongs to the area. $\alpha \geq 1$ is the parameter that controls the spread of membership degrees. In general, when α is close to 1, the centroids of n clusters tend to be distributed uniformly, whereas a large α gives centroids more concentrated on the center of the whole area. In other words, if α is too large, the membership degrees of the points located far from the center have similar values across all clusters. In our application, this may result in the overlap of exploration areas and increase the risk of flight path crossing. To minimize this risk, we choose α values that are close to 1. Given α, a heuristic solution method for this minimization problem yields the membership degree matrix $\boldsymbol{U}$ and the centroids vector $\boldsymbol{p}_\mathrm{a}$ [10], as shown in **Algorithm 1**.

3.2. Energy Constraint-Free Multiple TSP

Based on the results obtained from the fuzzy c-means clustering, we assign the set of points whose membership degrees of area k are above a certain threshold $\beta \in [0,1]$ as the initial measurement area covered by drone k, which is:

$$\mathscr{M}_k^{(0)} = \{i \in \mathscr{M} \,|\, u_{ki} \geq \beta\}, \quad \ldots\ldots\ldots (6)$$

where β is selected so that the following conditions hold:

$$\mathscr{M}_k^{(0)} \cap \mathscr{M}_\ell^{(0)} = \emptyset \quad \forall k \neq \ell \quad \ldots\ldots\ldots (7)$$

$$\bigcup_{k=1}^{n} \mathscr{M}_k^{(0)} \neq \mathscr{M}. \quad \ldots\ldots\ldots (8)$$

Condition (7) ensures that no point is visited by more than one drone, while condition (8) allows more flexibility for path generation so as to better account for energy consumption. The larger the value of β, the more points remain unassigned, which leaves room for energy equalization at a later stage of the algorithm.

Once the initial areas are assigned to the drones, the TSP[1] is solved for each initial area $\mathscr{M}_k^{(0)}$, $k = 1, \ldots, n$, and the corresponding energy consumption E_k of each drone is computed. Then, we iteratively distribute the points in $\mathscr{M} \setminus \bigcup_{k=1}^{n} \mathscr{M}_k$, i.e., the ones not yet assigned to any drone, to an appropriate cluster, to achieve energy consumption equalization. More specifically, if drone ℓ returns the minimum energy consumption among all the drones, the unassigned point with the highest membership to area ℓ is assigned to area ℓ. This process is repeated until all measurement points are assigned; the details are provided in **Algorithm 2**.

The results of point allocation to each drone could be manipulated by selecting appropriate α, β, and γ. However, it is still difficult to allocate the points located at the corners of the survey area to an appropriate drone. This motivates the introduction of the weights, w_i, as in Eq. (3).

Algorithm 1 Fuzzy c-means clustering (adapted from [10]).

Input Initial $\boldsymbol{U}^{(0)}$ satisfying $\sum_{k=1}^{n} u_{ki} = 1$
Area geometry coefficient $\gamma \geq 1$

Output Membership degree matrix $\boldsymbol{U} = [u_{ki}]$
Centroids vector $\boldsymbol{p}_\mathrm{a} = [\boldsymbol{p}_{\mathrm{a},k}]$

Repeat for $s = 1, 2, \ldots$

Step **1.1** Set the centroid of area k as

$$\boldsymbol{p}_{\mathrm{a},k}^{(s)} = \gamma \frac{\sum_{i=1}^{N} \left(u_{ki}^{(s-1)}\right)^\alpha \boldsymbol{p}_{\mathrm{m},i} w_i}{\sum_{i=1}^{N} \left(u_{ki}^{(s-1)}\right)^\alpha}, \quad k = 1, \ldots, n,$$

$$\text{where } w_i \coloneqq \frac{\|\boldsymbol{p}_{m,i}\|}{\sum_{j=1}^{N} \|\boldsymbol{p}_{m,j}\|} \quad \ldots\ldots\ldots\ldots (3)$$

Step **1.2** Set membership degree of point i to area k as

$$u_{ki}^{(s)} = \frac{1}{\sum_{l=1}^{n} \left(\dfrac{\|\boldsymbol{p}_{\mathrm{m},i} - \boldsymbol{p}_{\mathrm{a},k}^{(s)}\|}{\|\boldsymbol{p}_{\mathrm{m},i} - \boldsymbol{p}_{\mathrm{a},l}^{(s)}\|} \right)^{\frac{1}{\alpha-1}}}, \quad \begin{matrix} k = 1, \ldots, n \\ i = 1, \ldots, N \end{matrix}$$

normalizing $u_{ki}^{(s)} \leftarrow \frac{u_{ki}^{(s)}}{\sum_{\ell=1}^{n} u_{\ell i}^{(s)}}$, $i = 1, \ldots, n$, so as to ensure

$$u_{ki}^{(s)} \in [0,1] \quad \text{and} \quad \sum_{k=1}^{n} u_{ki}^{(s)} = 1 \quad \ldots\ldots (4)$$

Step **1.3** If the condition

$$\sum_{i=1}^{N}\sum_{k=1}^{n} \left\| u_{ki}^{(s)} - u_{ki}^{(s-1)} \right\| \leq \varepsilon \quad \ldots\ldots\ldots (5)$$

is satisfied, **return** $\boldsymbol{U} \leftarrow [u_{ki}^{(s)}]$ and $\boldsymbol{p}_\mathrm{a} \leftarrow [\boldsymbol{p}_{\mathrm{a},k}^{(s)}]$

---

1. Any standard TSP solution method can be used for this purpose. In this study, we employed a zero-one integer programming with iterative subtour-elimination process in the subsequent section for numerical simulations. The computation time was about 10 s for all the examples, using the following computer settings: AMD Ryzen 5 3600 with 6 CPU cores, 3.60 GHz base clock, and 16 GB RAM.

Algorithm 2 Multiple TSP.

Input Membership matrix $\boldsymbol{U} = [u_{ki}]$ from **Algorithm 1**

Output Measurement areas $(\mathscr{M}_k)$
Optimal paths $(\boldsymbol{\pi}_k)$

Step **2.1** Set the initial area $\mathscr{M}_k^{(0)}$ for each drone $k = 1,\dots,n$ as in Eq. (6) with β chosen so that Eqs. (7) and (8) hold

Step **2.2** For each initial area $\mathscr{M}_k^{(0)}$, $k = 1,\dots,n$, compute optimal path $\boldsymbol{\pi}_k^{(0)}$ by solving a TSP and compute the energy consumption E_k of drone k as in Eq. (2a)

Repeat for $t = 0, 1, \dots$

Step **2.3** If $\bigcup_{k=1}^{n} \mathscr{M}_k^{(t)} = \mathscr{M}$ (all points are assigned) **return** $(\mathscr{M}_k) \leftarrow (\mathscr{M}_k^{(t)})$ and $(\boldsymbol{\pi}_k) \leftarrow (\boldsymbol{\pi}_k^{(t)})$

Step **2.4** Select drone $\ell \in \arg\min_{k\in\mathscr{D}} E_k$ and an unassigned point $j \in \arg\max_{i\in\mathscr{M}\setminus\bigcup_{k=1}^{n}\mathscr{M}_k^{(t)}} u_{\ell i}$, and leave

$$\mathscr{M}_k^{(t+1)} = \mathscr{M}_k^{(t)} \text{ and } \boldsymbol{\pi}_k^{(t+1)} = \boldsymbol{\pi}_k^{(t)} \quad \forall k \neq \ell$$

Step **2.5** Solve a TSP on area $\mathscr{M}_\ell^{(t+1)} = \mathscr{M}_\ell^{(t)} \cup \{j\}$ to compute an optimal path $\boldsymbol{\pi}_\ell^{(t+1)}$, and update the energy consumption E_ℓ of drone ℓ as in Eq. (2a)

Algorithm 3 Seismic survey protocol of drone k.

Input Area $\mathscr{M}_k$ and path $\boldsymbol{\pi}_k = (\boldsymbol{\pi}_{k,1},\dots,\boldsymbol{\pi}_{k,|\mathscr{M}_k|})$ from **Algorithm 2**

While $\mathscr{M}_k \neq \emptyset$

Step **3.1** Perform the survey along the first $i_{\max}$ points of path $\boldsymbol{\pi}_k$, where $i_{\max}$ is as in Eq. (9)

Step **3.2** Redefine $\mathscr{M}_k \leftarrow \mathscr{M}_k \setminus \{\boldsymbol{\pi}_{k,1},\dots,\boldsymbol{\pi}_{k,i_{\max}}\}$ and recompute $\boldsymbol{\pi}_k$ by solving the TSP for $\mathscr{M}_k \cup \{0\}$

3.3. Individual Path Optimization with Battery Recharging

Using the solution method proposed in **Algorithm 2**, we obtain an upper bound on the required number of drones to complete the survey. In this subsection, we consider the case where the number of available drones is less than this upper bound, which means that, to complete the task, drones need to return to the depot for recharging their batteries.

In contrast to **Algorithms 1** and **2**, this last stage can be accomplished in parallel by each drone as the measurement areas are pairwise disjoint and remain unchanged. In other words, each drone $k \in \mathscr{D}$ will individually implement the proposed **Algorithm 3** based on its measurement area $\mathscr{M}_k$ and optimal TSP path $\boldsymbol{\pi}_k$ retrieved in **Algorithm 2**. The rationale behind this is as follows.

If the drone has sufficient battery to pass through all the measurement points in $\boldsymbol{\pi}_k$ and return to the depot, then it simply performs the entire route and terminates. Otherwise, it only visits as many points as it can survey along $\boldsymbol{\pi}_k$ without compromising a safe return to the depot. Once this partial survey is completed, the visited points are removed from area $\mathscr{M}_k$, and a new (single-agent) TSP is solved to update the optimal path $\boldsymbol{\pi}_k$. After this, the process is repeated as many times as needed until all points have been visited. The number of points that can be surveyed in one round is given by:

$$i_{\max} \coloneqq \arg\max \left\{ i | E_{k,i}^{\boldsymbol{\pi}_k} \leq E_k^{\max} \right\}, \quad \dots\dots \quad (9)$$

where $E_{k,i}^{\boldsymbol{\pi}_k}$ denotes the energy consumption of drone k for visiting the first i points of path $\boldsymbol{\pi}_k$ and returning to the depot, and $E_k^{\max}$ is the maximum energy that drone k has available to operate. The overall process is synopsized in **Algorithm 3**. Note that $i_{\max}$ is well defined, provided that each drone has enough energy to travel (at least) to any point, perform the survey there, and return to the depot. Thus, this condition is thus assumed throughout.

The time required to charge a battery does not affect the solutions found because the cost function is given by the energy required to visit all points, take measurements and return to the depot. However, this does affect the total survey time. Hence, returning to the depot before fully depleting the batteries may prove to be more efficient. Different strategies that consider the optimization of total survey time are being considered for future work. In a special case, where the charging time is negligible (such as when batteries are directly replaced), there is a strong correlation between our solutions and short survey times, as mentioned in Section 1.

4. Simulations

In this section, we demonstrate the efficacy of a sequential implementation of **Algorithms 1**, **2**, and **3** through numerical simulations. We consider a survey area of 1×1 km^2 for a surface wave analysis with $N = 100$ measurement points. We assume that the depot and the seismic source are both located at the center of the area. This is a standard assumption in practice: i) since various devices such as data loggers are also placed near the seismic source, it is natural to use this location for the depot; and ii) because a GPS clock is used together with the seismic source, an open-sky location is commonly chosen, which is also appropriate for a drone base. Placing the seismic source at the center is also reasonable because of its energy efficiency; if placed in a corner, the distance to the furthest seismometer would increase, hence requiring a larger seismic source. Regardless, the algorithm can also cope with arbitrary positions of the depot and the seismic source by modifying the weights w_i and area geometry coefficient γ in **Algorithm 1**.

The chosen drone model was a Phantom 4 Pro of DJI, its specifications of which are listed in **Table 1**.[2] Its battery power capacity of 89.2 Wh is then converted to the battery capacity $E_{k,\max}$ of 321.1 kJ for any $k \in \mathscr{D}$.

The energy consumption of each flight mode, E_k^{up},

2. https://www.dji.com/phantom-4-pro/info#specs [Accessed December 1, 2021]

Table 1. Specifications of the drone Phantom 4 Pro.

Maximum ascent speed	6.0 m/s
Maximum descent speed	4.0 m/s
Maximum forward speed	5.6 m/s
Battery power capacity	89.2 Wh

Table 2. Energy consumption of drone k to move from point i to point j per flight mode in Eq. (1).

E_k^{up}	$29.7(2k-1.5)$ [J]
E_{ij}^{fwd}	$32.1\|p_{\text{m},i} - p_{\text{m},j}\|$ [J]
E_k^{down}	$356.8(2k-1.5)$ [J]
E_j^{idle}	$600t_j$ [J]

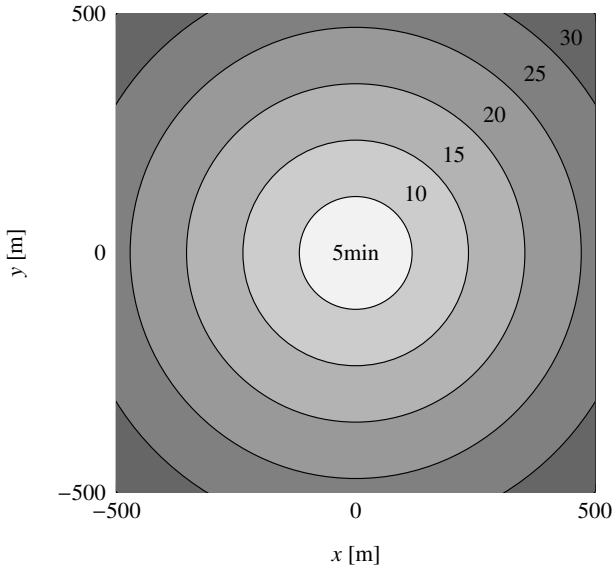

Fig. 4. Required drone idling time in the survey area, based on the distance from the seismic source.

E_{ij}^{fwd}, E_k^{down}, and E_j^{idle} is calculated based on the values reported by [14] and listed in **Table 2**. E_k^{up} and E_k^{down} are set differently for each drone so as to avoid collisions, using a 2 m gap between each drone, starting from 0.5 m. t_j [min] in E_j^{idle} denotes the measurement time required at point j while the drone is idle. As previously mentioned, the required measurement time is inversely proportional to the distance from the seismic source. We set the time as in **Fig. 4**, where the seismic source is located at the origin, i.e., for $a = 1,\ldots,6$ and $d_{\max} = 500\sqrt{2}$ m. t_j is given by:

$$t_j = 5a \quad \text{for} \quad \frac{a-1}{6}d_{\max} < \|p_{m,j}\| \leq \frac{a}{6}d_{\max}.$$

4.1. Without Battery Recharging

We start by considering the case where plenty of drones for the survey exist. Using **Algorithms 1** and **2**, we find that the smallest number of drones required to complete the survey without recharging the battery is $n^* = 5$. **Fig. 5(a)** shows the paths obtained for $n = 5$ by setting the parameters α, β, and γ in **Algorithm 1** as $\alpha = 1.35$, $\beta = 0.6$, and $\gamma = 1.4$. As shown in the table therein, all the drones satisfy the battery constraint $E_k \leq E_k^{\max} = 321.1$ kJ. We also note that the energy consumption is approximately the same among all the drones, which is ideal to attain the shortest completion time.

Remark. In [8], a numerical study was conducted for a similar setting with the only difference being the idling time, which was set to 30 min at all the measurement points. The value of n^* was computed as 9, which is almost double the number obtained in this study.

4.2. With Battery Recharging

The final case we look at considers that the number of available drones is less than the minimum number required to complete the entire survey without any drone recharging its battery. Here, we set $n = 3 < n^*$. **Fig. 5(b)** shows that the paths obtained by **Algorithms 1** and **2** for $\alpha = 1.1$, $\beta = 0.8$, and $\gamma = 1.4$, i.e., without considering the energy consumed, resulting in all the drones violating the battery constraint $E_k \leq E_k^{\max} = 321.1$ kJ. The paths in **Fig. 5(c)** are instead obtained by a subsequent application of **Algorithm 3**, which, to account for battery limitation, recommends two loops for each drone to fully complete the task.

5. Conclusion

Herein, we propose a heuristic algorithm that can generate energy-minimizing paths for multiple drones, operating in tandem to conduct a seismic survey by carrying a seismometer and taking measurements at points distributed across a large area. The need for each drone to remain idle at measurement points over varying periods of time, depending on the proximity to the seismic source, leads to the energy consumption not being proportional to path length. This variation of the optimization algorithm was not yet available for this specific application. To address it, we extended the algorithm proposed by [9] to approximately solve a standard mTSP problem while attempting to equalize the path length between salesmen. Finally, to account for the limited battery capacity of each drone, the algorithm was further enhanced with a final step that prescribes the optimum return routes for recharging of each drone based on their individual capacity. Numerical simulations demonstrated the validity of the proposed algorithms for their use in automated seismic surveys.

We note that this study considered a surface wave analysis. In this case, only one seismic source at a fixed position is sufficient. However, if body wave information is

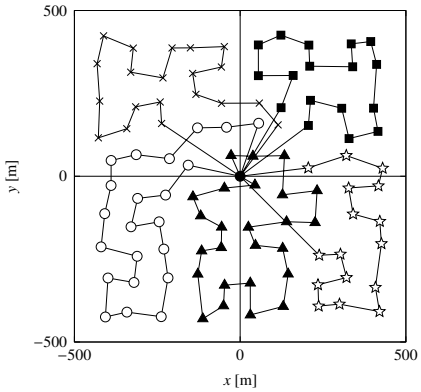

(a) Output of **Algorithm 2** with $n = 5$. Five drones are enough to complete the whole task without recharging the battery.

Drone k	$\mathscr{M}_k$	E_k [kJ]
Drone 1	○	306.5
Drone 2	×	310.0
Drone 3	▲	301.5
Drone 4	■	304.8
Drone 5	☆	303.9

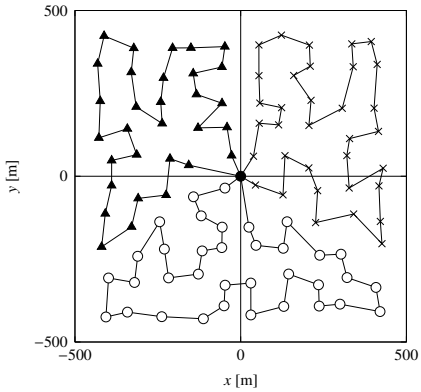

(b) Output of **Algorithm 2** with $n = 3$. The energy required to survey all points exceeds each drone's capacity.

Drone k	$\mathscr{M}_k$	E_k [kJ]
Drone 1	○	470.2
Drone 2	×	468.0
Drone 3	▲	467.8

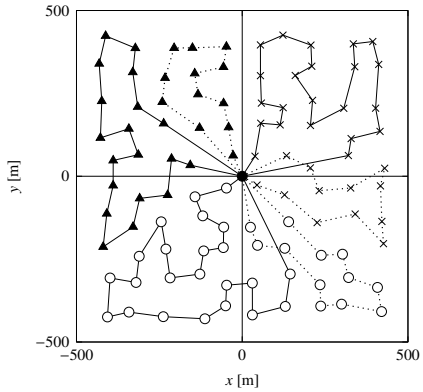

(c) Output of **Algorithm 3** with $n = 3$. By recharging once, two loops (solid and dotted lines) suffice to complete the survey.

Drone k	$\mathscr{M}_k$	E_k [kJ] per loop	
Drone 1	○	310.9	174.5
Drone 2	×	309.0	163.1
Drone 3	▲	313.9	165.4

Fig. 5. Comparison of the optimal paths for different numbers of available drones with/without battery recharging. The energy consumption detailed in the tables shows how the equalizing effect of **Algorithm 2** is inherited by each path generated by **Algorithm 3**.

required for the seismic surveys (e.g., in seismic reflection or refraction surveys), the seismic source would also need to migrate during the process. Recently, a new seismic source has been developed that is sufficiently small to be mounted on a drone [3]. This offers a promising direction for future studies in this field, by developing further algorithms that can optimize both seismic-source migration and measurements using multiple drones.

Through the numerical studies, it also became apparent that the drone energy consumption due to the mandatory idling time is significant. Therefore, the use of a commercial drone for this purpose may not be the best choice, but instead the development of a drone with much lower energy consumption while idling may be more suitable for practical use in seismic surveys.

Acknowledgments

This work was partly supported by JSPS KAKENHI Grant Numbers JP20K14766, JP20H01997, and JP22H05108.

References:

[1] T. Ikeda, T. Tsuji, M. Nakatsukasa, H. Ban, A. Kato, K. Worth, D. White, and B. Roberts, "Imaging and monitoring of the shallow subsurface using spatially windowed surface-wave analysis with a single permanent seismic source," Geophys., Vol.83, No.6, pp. EN23-EN38, 2018.

[2] T. Tsuji, J. Kinoshita, S. Tsuji, K. Yamamoto, and T. Ikeda, "Drone-based active-source multichannel seismic survey system," Summit on Drone Geophysics, 2021.

[3] T. Tsuji, S. Tsuji, J. Kinoshita, T. Ikeda, and A. Ahmad, "4 cm Portable Active Seismic Source (PASS) for Meter-to Kilometer-Scale Imaging and Monitoring of Subsurface Structures," Seismol. Res. Lett., 2022.

[4] S. Anily and G. Mosheiov, "The traveling salesman problem with delivery and backhauls," Oper. Res. Lett., Vol.16, No.1, pp. 11-18, 1994.

[5] H. Jin, Q. He, M. He, F. Hu, and S. Lu, "New method of path optimization for medical logistics robots," J. Robot. Mechatron., Vol.33, No.4. pp. 944-954, 2021.

[6] S. Cavani, M. Iori, and R. Roberti, "Exact methods for the traveling salesman problem with multiple drones," Transp. Res. Part C: Emerg. Technol., Vol.130, Article No.103280, 2021.

[7] S. Kim and I. Moon, "Traveling salesman problem with a drone station," IEEE Trans. Syst., Man, Cybernet.: Syst., Vol.49, No.1, pp. 42-52, 2018.

[8] Y. Hamasato, A. Sakaguchi, K. Yamamoto, and T. Tsuji, "Multiple drone route optimization for a seismic survey," Trans. Inst. Syst., Control Inf. Eng., 2023 (in press) (in Japanese).

[9] H. Watanabe, T. Ono, A. Matsunaga, and A. Kanagawa, "Multiple traveling salesman problems using the fuzzy c-means clustering," J. Japan Soc. Fuzzy Theory Syst., Vol.13, No.2, pp. 119-126, 2001 (in Japanese).

[10] J. Bezdek, "Pattern recognition with fuzzy objective function algorithms," Plenum Press, 1981.

[11] T. Bektas, "The multiple traveling salesman problem: an overview of formulations and solution procedures," Omega, Vol.34, No.3, pp. 209-219, 2006.

[12] K. Bérczi, M. Mnich, and R. Vincze, "Approximations for Many-Visits Multiple Traveling Salesman Problems," Omega, Article No.102816, 2022.

[13] O. Cheikhrouhou and I. Khoufi, "A comprehensive survey on the Multiple Traveling Salesman Problem: Applications, approaches and taxonomy," Comput. Sci. Rev., Vol.40, Article No.100369, 2021.

[14] R. Alyassi, M. Khonji, A. Karapetyan, S. Chau, K. Elbassioni, and C. Tseng, "Autonomous recharging and flight mission planning for battery-operated autonomous drones," IEEE Trans. Autom. Sci. Eng., 2022.

Name:
Yohei Hamasato

Affiliation:
Graduate School of Information Science and Electrical Engineering, Kyushu University

Address:
744 Motooka, Nishi-ku, Fukuoka 819-0395, Japan

Brief Biographical History:
2017- Undergraduate Student, Kyushu University
2021- Graduate Student, Kyushu University

Main Works:
• "Multiple drone route optimization for a seismic survey," Trans. of the Institute of Systems, Control and Information Engineers, 2023 (in press).

Membership in Academic Societies:
• The Institute of Systems, Control and Information Engineers (ISCIE)

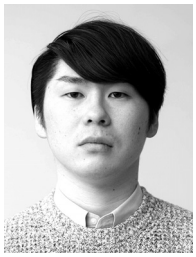

Name:
Akinori Sakaguchi

ORCID:
0000-0003-1895-9570

Affiliation:
Project Assistant Professor, Research Institute of Advanced Electric Propulsion Aircrafts, Kyushu University

Address:
744 Motooka, Nishi-ku, Fukuoka 819-0395, Japan

Brief Biographical History:
2021 Received Doctoral degree from Osaka University
2021 Postdoctoral Researcher, Kyushu University
2022- Project Assistant Professor, Kyushu University

Main Works:
• "A Novel Quadrotor with a 3-axis Deformable Frame using Tilting Motions of Parallel Link Modules without Thrust Loss," IEEE Robotics and Automation Letters, Vol.7, No.4, pp. 9581-9588, 2022.

Membership in Academic Societies:
• Institute of Electrical and Electronics Engineers (IEEE)
• The Robotics Society of Japan (RSJ)
• The Japan Society of Mechanical Engineers (JSME)

Name:
Takeshi Tsuji

ORCID:
0000-0003-0951-4596

Affiliation:
Professor, Department of Systems Innovation, Graduate School of Engineering, The University of Tokyo

Address:
7-3-1 Hongo, Bunkyo-ku, Tokyo 113-8656, Japan

Brief Biographical History:
2007 Received Ph.D. degree from The University of Tokyo
2007- Assistant Professor, Kyoto University
2012- Associate Professor, Kyushu University
2017- Professor, Kyushu University
2022- Professor, The University of Tokyo

Main Works:
• "4 cm portable active seismic source (PASS) for meter- to kilometer-scale imaging and monitoring of subsurface structures," Seismological Research Letters, Vol.94, No.1, pp. 149-158, 2023.
• "Continuous monitoring system for safe managements of CO2 storage and geothermal reservoirs," Scientific Reports, Vol.11, Article No.19120, 2021.

Membership in Academic Societies:
• Japan Geoscience Union (JpGU)
• Society of Exploration Geophysicists (SEG)
• American Geophysical Union (AGU)

Name:
Kaoru Yamamoto

ORCID:
0000-0003-1888-3529

Affiliation:
Associate Professor, Faculty of Information Science and Electrical Engineering, Kyushu University

Address:
744 Motooka, Nishi-ku, Fukuoka 819-0395, Japan

Brief Biographical History:
2016 Received Ph.D. degree from University of Cambridge
2016 Postdoctoral Researcher, University of Minnesota Twin Cities
2017 Postdoctoral Researcher, Lund University
2018- Associate Professor, Kyushu University

Main Works:
• "Hypertracking and Hyperrejection: Control of Signals beyond the Nyquist Frequency," IEEE Trans. on Automatic Control, 2022 (advance online publication). https://doi.org/10.1109/TAC.2022.3230599
• "Bounded Disturbance Amplification for Mass Chains with Passive Interconnection," IEEE Trans. on Automatic Control, Vol.61, No.6, pp. 1565-1574, 2016.

Membership in Academic Societies:
• Institute of Electrical and Electronics Engineers (IEEE)
• The Society of Instrument and Control Engineers (SICE)
• The Robotics Society of Japan (RSJ)